NEUROPHOTONICS

REVIEW

Advances in cellular resolution microscopy for brain imaging in rats

Su Jin Kim,[a] **Rifqi O. Affan**,[b,c] **Hadas Frostig**,[b] **Benjamin B. Scott**,[b,d,*] **and Andrew S. Alexander**[e]

[a]Johns Hopkins University, Department of Psychological and Brain Sciences, Baltimore, Maryland, United States

[b]Boston University, Center for Systems Neuroscience, Department of Psychological and Brain Sciences, Boston, Massachusetts, United States

[c]Boston University, Graduate Program in Neuroscience, Boston, Massachusetts, United States

[d]Boston University, Neurophotonics Center and Photonics Center, Boston, Massachusetts, United States

[e]University of California Santa Barbara, Department of Psychological and Brain Sciences, Santa Barbara, California, United States

ABSTRACT. Rats are used in neuroscience research because of their physiological similarities with humans and accessibility as model organisms, trainability, and behavioral repertoire. In particular, rats perform a wide range of sophisticated social, cognitive, motor, and learning behaviors within the contexts of both naturalistic and laboratory environments. Further progress in neuroscience can be facilitated by using advanced imaging methods to measure the complex neural and physiological processes during behavior in rats. However, compared with the mouse, the rat nervous system offers a set of challenges, such as larger brain size, decreased neuron density, and difficulty with head restraint. Here, we review recent advances in *in vivo* imaging techniques in rats with a special focus on open-source solutions for calcium imaging. Finally, we provide suggestions for both users and developers of *in vivo* imaging systems for rats.

Keywords: calcium; head-mounted; two-photon imaging; multiphoton; behavior; cortex; rat; brain imaging; *in vivo* imaging

Paper 23036SSVR received May 5, 2023; revised Sep. 23, 2023; accepted Nov. 7, 2023; published Nov. 30, 2023.

1 Introduction

Advances in genetically encoded sensors provide increased sensitivity, cell type specificity, and the ability to record a variety of signals from intracellular calcium[1] and membrane voltage,[2] to neurotransmitter release such as dopamine.[3,4] New microscopes have been developed to image across larger areas, with greater resolution, increased depth, and enhanced portability.[5–7] These methods are being increasingly paired with sophisticated analytical techniques, which have opened new avenues within theoretical neuroscience.[8–10]

The development of *in vivo* cellular resolution imaging technologies, and calcium imaging in particular, has been one of the modern success stories in systems neuroscience.[11] Over the past 60 years, these tools have been applied to a variety of model organisms [Fig. 1(a)]. However, in the last 15 years, the mouse has emerged as a leading model for *in vivo* cellular resolution imaging. This is likely due to the confluence of genetic tools, such as transgenic mouse lines (e.g., Ref. 23), and methods that enable imaging during behavior, such as head-fixed virtual reality (VR[16]) and head mounted microscopes.[17]

*Address all correspondence to Benjamin B. Scott, bbs@bu.edu

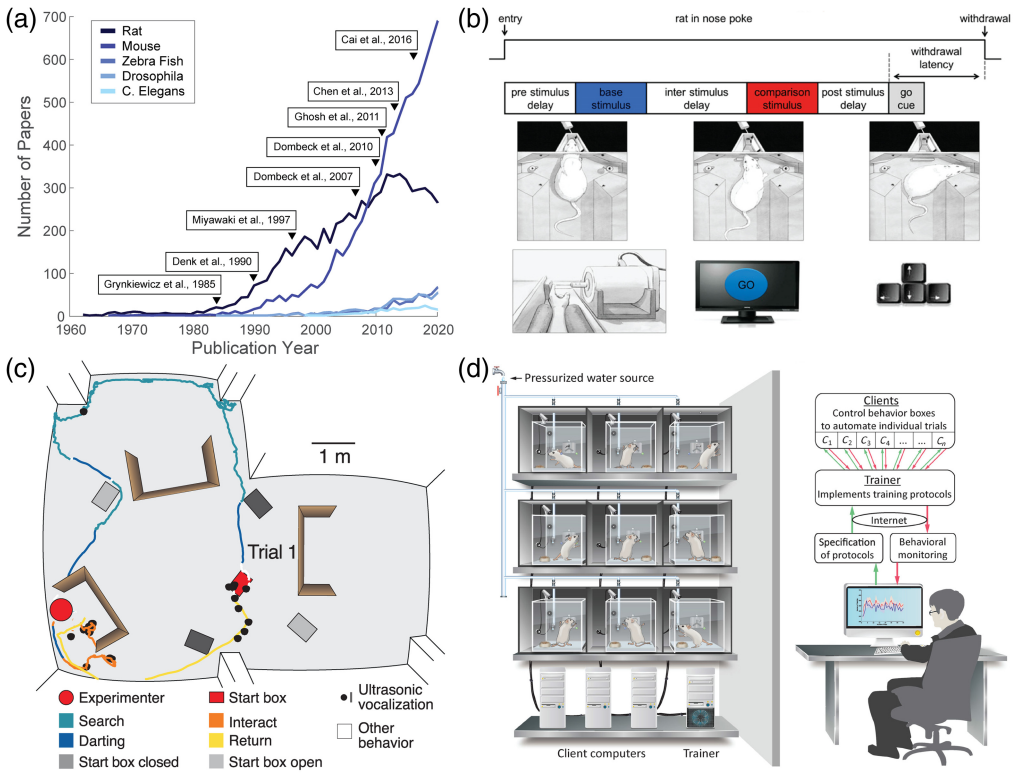

Fig. 1 Tasks and behavioral control systems used in rats. (a) Number of papers on PubMed by year with the search term "calcium imaging" and either "rat," "mouse," "zebrafish," "drosophila," or "*Caenorhabditis elegans*" from 1964 to 2019. Key calcium imaging papers are denoted by a triangle and the citation: development of fura-2, a fluorescent dye to detect calcium,[12] the first 2P microscope,[13] development of an early genetically encoded calcium sensor,[14] a treadmill system for *in vivo* imaging,[15] the first VR system used with 2P imaging in mice,[16] wearable epifluorescent microscope,[17] development of GCaMP6,[18] and development of the open-source miniscope.[19] (b) Schematic of a tactile comparison task to measure parametric working memory (top), with rats (middle) and humans (bottom) performing the task.[20] (c) Trajectory of a hide-and-seek task trial in rats, where the rat emerges from the start box and searches for the human experimenter.[21] (d) A fully automated, live-in facility for rat behavioral training.[22]

While success of *in vivo* imaging technologies in mice has inspired the field, progress in other organisms, including rats, continues. Rats have historically been an important model for biomedical and neuroscience research (Refs. 24 and 25; see Table 1). Today they remain a leading model for studying neural dynamics during complex learned behaviors, such as navigation,

Table 1 Pioneering discoveries in systems neuroscience using the rat model.

Discovery	Reference(s)
Adult neurogenesis	Altman and Das[26]
Place cells	O'Keefe and Dostrovsky[27]
Head direction cells	Taube et al.[28]
First BOLD measurement with fMRI	Ogawa et al.[29]
Odorant receptor gene	Buck and Axel[30]
Neural replay	Wilson and McNaughton[31]
In vivo 2P imaging	Denk et al.[32]
Grid cells	Hafting et al.[33]

decision making, and addiction. The behavioral advantages of this organism have motivated continued innovation in applying calcium imaging tools. Recent successes reflect this: new imaging technologies for rats include multiphoton microscopy using voluntary head restraint,[34,35] open-source widefield microscopes for large field of view (FOV) recording,[36,37] head mounted three photon (3P) microscopes,[38] and transgenic rats expressing calcium indicators.[34,37]

Given the significance of the rat animal model in neuroscience and neuroimaging specifically, continued development of *in vivo* imaging tools in this species is warranted. This review will focus on specific opportunities and challenges posed by neuroimaging in the rat model, describe the technical solutions under development, and provide an outlook for technologies that may facilitate future imaging experiments.

2 Opportunities in Rat Imaging

The rat model has advantages that motivate its continued use for studying the link between cellular dynamics and behavior. In this section, we provide an overview of these advantages and the experimental opportunities of the rat model system.

2.1 Behavioral Repertoire

Rats distinguish themselves as model organisms because of their complex behavioral repertoire, adaptability, and the variety of tools to study both learned and natural behaviors. Rats can be trained on a wide range of tasks designed to characterize goal-directed behaviors and decision-making.[39–43] For example, rats can readily learn to perform parametric working memory tasks inspired by primate tasks[20,44] [Fig. 1(b)] and can learn the representation of action-outcome associations in a multi-step planning tasks.[45,46] Rats can learn behavioral paradigms originally developed for humans, facilitating comparative studies and translational research in neuropsychiatry.[47,48] Rats are also social creatures,[49] demonstrating pro-social behaviors in controlled laboratory environments,[50,51] including empathy,[52] cross species play[21] [Fig. 1(c)], and collaborative group search.[53]

The wide range of behavioral features in rats contribute to their usefulness as a model organism for basic and translational neuroscience research. Unfortunately, direct, quantitative comparisons of behaviors between rats and other model organisms, in particular mice, is rarely performed, and this limitation is particularly acute in complex decision-making tasks, which are presently of great interest.[54] Ethological behaviors are somewhat conserved; mice and rats have similar aggression, grooming, feeding, and reproductive behaviors.[55] While the overall behavioral patterns are consistent between species, there are slight nuances to many of these innate behaviors (e.g., rats exhibit more complex grooming phases than mice). A quantitative comparison between rat and mouse behavior across a range of tasks would facilitate an unbiased assessment of the pros and cons of each species. In some cases, such as addiction, these side-by-side comparisons have been performed. For example, there is some indication that rats are a better model for studying alcohol relapse behaviors than mice.[56]

Numerous open-source tools and pipelines have been developed for behavioral training and measurement in rats. These include VR navigation systems[57–59] automated operant systems[22,39] [Fig. 1(d)], touchscreen training,[60] and voluntary head restraint.[61–63] Together, the availability of experimental and computational tools for behavioral research in rats provides frameworks for collecting and analyzing high-throughput data in a variety of laboratory settings, which can easily be paired with multimodal imaging approaches.[64]

2.2 Body Size

Adult rats weigh hundreds of grams (250 to 350 g for a 10 week old male Long Evans)[65] and have significant capacity for implantable and wearable devices. Rats can carry head mounted devices weighing 35 g while still displaying natural behaviors, such as rearing and rapid head orienting.[37] This capacity reduces constraints on development allowing for microscopes with larger FOVs[36,37] and or more complex optical components.[66] Beyond the rat's physical strength, the larger size and rectilinear shape of the skull provides ample "real estate" for device attachment.

Beyond the technological advantages that rats provide because of their physiology, rats can also act as a bridge to larger model organisms for neuroscientific research. As we describe below,

the brains of larger animals pose challenges to imaging, which will require new imaging capabilities. Rats, with their relatively wide range of available transgenic lines and genetic tools, may provide a valuable test case for developing and expanding technology for other animals, such as ferrets, macaques, and marmosets.

3 Challenges in Rat Imaging

3.1 Head Restraint

Head restraint is widely used in neuroscience to stabilize the brain position relative to the imaging apparatus. Head restraint in rats can be accomplished through an acclimation process in which the duration of restraint is gradually increased.[67] However, compared with mice, this approach is unreliable and more limited in rats—they show increased stress and diminished behavioral flexibility during head restraint.[68] Consequently, forced head restraint is not frequently used in conjunction with complex cognitive task learning in rats. This has motivated the development of head-mounted microscopes and voluntary head-fixation (see Sec. 4).

3.2 Decreased Neuronal Density

While being 8 to 10 times the body mass of mice, rats have three times the number of neurons; much of this increase in neurons is in the cerebellum, and the fraction of cortical neurons remains constant even as total brain size increases.[69–71] Mice have on average 78,672 neurons and 68,640 nonneuronal cells per milligram of cortical tissue, whereas rats have 41,092 neurons and 60,430 nonneuronal cells per milligram.[69] In terms of density, rats have half the number of neurons per milligram of cerebral cortex compared with mice.[70,72] Lower neuron densities will result in fewer imaged neurons when assuming the same FOV and signal-to-noise ratio (SNR). This challenge is not unique to rats—it is a challenge shared by many larger-brained animals, including several primate species.[69,70,73]

3.3 Increased Cortical Thickness

The rat neocortex is thicker than the mouse neocortex; for example, the motor cortex of rats has an average thickness of 1.6 mm while in mice motor cortex has an average thickness of 1.0 mm.[71] Since the scattering length of the rat cortex is similar to that of the mouse,[32,74–78] the excitation light penetrates to a comparable depth in both animals. Overall, this results in reduced optical access into deeper layers in the rat brain. In most cases, cell somas in layer 2/3 of rat neocortex, which ranges from 200 to 500 μm,[79] can lie below the range of some head-mounted one-photon imaging systems[17] and makes imaging of infragranular layers difficult. To surpass these limitations, researchers can implant microprisms, relay gradient index (GRIN) lenses, or use 3P microscopy, all three of which we discuss in more detail in the following section (see Sec. 4).

3.4 Vascular Size and Branches

Rat brains have an increased number of capillary branches per unit volume and larger radii of vessels compared to mouse brains.[80,81] This can lead to changes in the optical properties of tissue, such as increased absorption of light at different wavelengths due to hemoglobin.[37,82–84] In addition, these differences in vasculature can contribute to difficulties in surgery (such as increased bleeding) when compared to mice.

3.5 Transgenesis

Tools for the production of transgenic rats are well developed and several lines of genetically modified rats that express calcium sensors have been produced (see Sec. 4). However, the costs, speed of generation, and number of off the shelf transgenic lines in mice greatly exceeds the rat model at present. The availability of transgenic lines is an important feature that should be considered when selecting a model organism for calcium imaging studies.

4 Tools for Rat Imaging

Below, we highlight the recent applications of imaging tools and labeling techniques in rats.

4.1 Transgenic Lines

Several useful transgenic lines for neuroscience and specifically *in vivo* imaging are available from several sources, including the Rat Resource and Research Center (RRRC) and the Rat Genome Database.[85] Available lines include Cre driver lines for cell type specific expression (e.g. Refs. 86 to 88) and genetic models for human neuropsychiatric disorders, such as models of autism.[89] The Rat Genome Database provides a valuable list of resources for the development of transgenic rats.[90]

Transgenic lines have also been developed that express genetically encoded calcium sensors for *in vivo* imaging[34,37] [Figs. 2(a)–2(c)]. These lines, created by Janelia Research Campus on the Long-Evans background, express the genetic calcium indicator GCaMP6f throughout large regions of the CNS, with different transgenic lines having clusters of expression in different areas.

Sensor expression in at least two transgenic rat strains, Thy-1-GCaMP6f-7 and Thy-1-GCaMP6f line 8, is sufficient for cellular resolution imaging through either one or two-photon (2P) microscopes.[34,37,92] However, the use of newer GCaMP variants delivered by adeno associated viral vectors (AAV) injection appears to provide improved SNR and action potential (AP) detection. For example, Chornyy et al.[93] found that single AP detection was detected in 10.6% (48/450) of GCaMP6f-labeled neurons labeled in Thy-1-GCaMP6f animals, whereas it was detected in ∼85% (412/485) of jGCaMP7s-positive cells labeled with AAVs. These results indicate that new GCaMP variants and/or viral labeling may improve signal detection.

4.2 Viral Vectors

At the time of writing, the majority of published studies involving imaging of genetically encoded sensors in rats express sensors using direct injection of AAVs[35,36,63,94–98] [Figs. 2(d) and 2(e)]. AAVs are favored due to the high-levels of expression that are difficult to obtain in transgenics[99] and the availability of new genetically encoded sensors, which are being developed more rapidly than new transgenic lines. Direct injection of high-titer viral vectors into the rat CNS is widely used to achieve local expression of genetically encoded sensors. To achieve more widespread expression, several alternative approaches have been explored. One method is using serial injections, which has been demonstrated across the rat cortex. In this approach, a series of injections are performed at regular increments, tiling a larger volume. This approach aims to achieve a more uniform labeling over a larger volume than could be achieved by a single injection [Figs. 2(d) and 2(e)].[67,88,100] Several groups have also reported widespread CNS infection in adults following systemic administration through intravenous,[101–103] intraventricular, and intrathecal injection.[104,105] These techniques reduce the potential for damage to neural tissue following direct injections. The efficiency of these techniques is enhanced by the development of enhanced AAV capsids (such as PHP.eB), which yield improved gene transfer in rat CNS.[104,106] While these approaches are intriguing, they have not been widely used in combination with *in vivo* functional imaging approaches in rats.

4.3 *In Utero* Gene Delivery

Another method for gene delivery used in rats is via *in utero* electroporation, a method for transfecting neural tissue with plasmid DNA via injection into embryonic brains [Figs. 2(f) and 2(g)]. *In utero* electroporation enables widespread expression in neurons throughout the CNS.[91,107–111] In addition, *in utero* AAV injections can be used to achieve widespread cortical labeling in rats.[112]

A strength of *in utero* gene delivery is that it can be implemented during different stages of development to yield spatially specific expression within the neocortex without the need for laminar specific promoters. Moreover, the method can be optimized to produce widespread infection from a single injection. That said, gene delivery to the rat embryo requires specialized techniques and equipment, and there is some indication that introduction of foreign genetic material during development can produce an immune response that alters or even damages the brain.[113]

4.4 Head-Mounted Microscopes Designed for Mice

Miniaturized head mounted epifluorescence microscopes allow recording of calcium dynamics in freely behaving animals.[17] This approach bypasses the problem of head restraint and stabilization while achieving cellular resolution imaging.[114] These microscopes have been widely

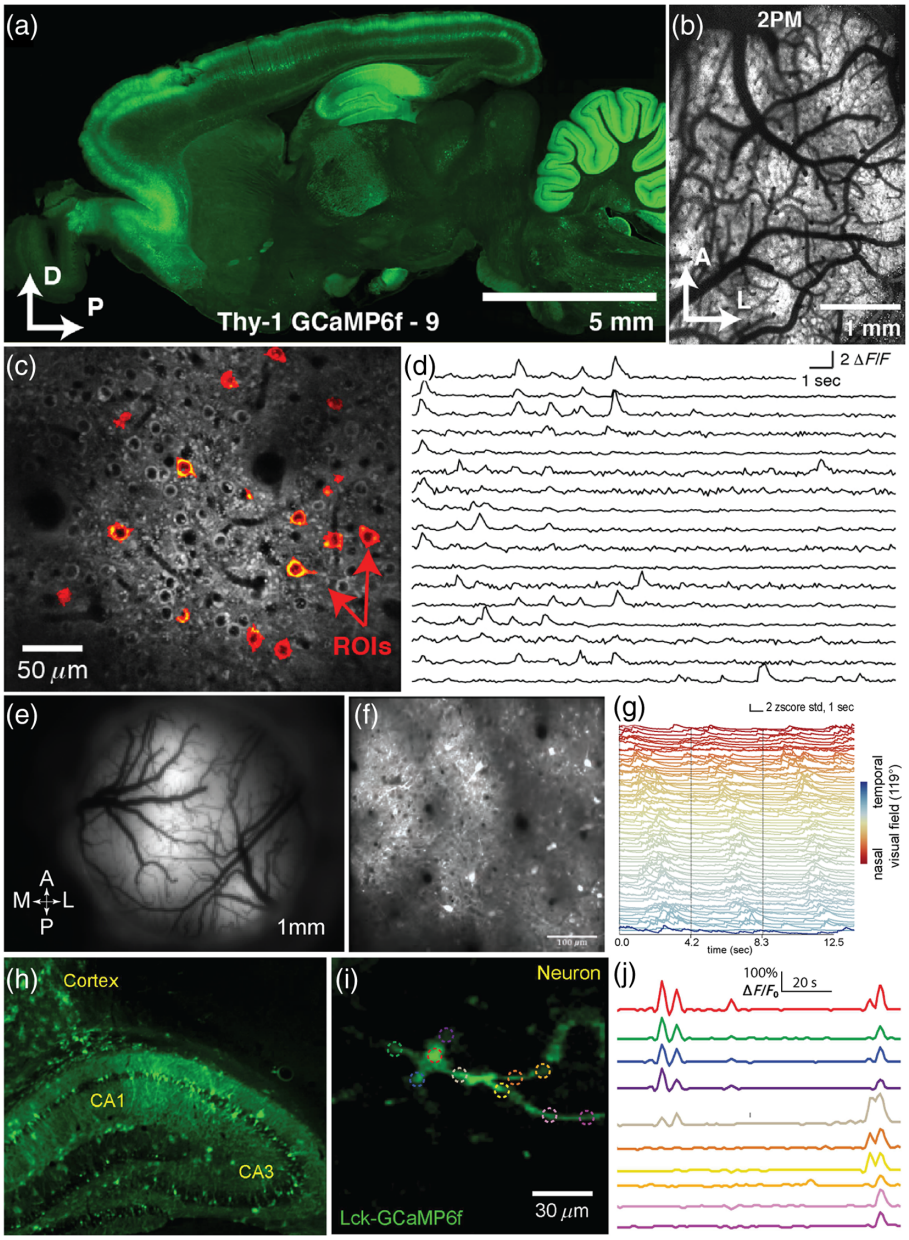

Fig. 2 Labeling systems for rats. (a) Sagittal section of a Thy1 GCaMP6f-9 rat (from Ref. 37). (b), (c) 2P imaging of layer 2/3 of the cerebral cortex of a transgenic rat expressing GCAMP6f, where red pixels identify ROIs.[37] (d) Calcium traces from the 17 ROIs in panel C at 30 Hz.[37] (e) Epifluorescence image of a cranial window in a rat following serial viral injections with AAV9-GCaMP7f.[67] (f) 2P imaging of a 500 μm × 500 μm FOV from rat cortex injected with GCaMP7f.[67] (g) *Z*-scored traces from the rat visual cortex for three cycles of presentation of a moving bar sweeping in the nasal-to-temporal direction at 0.24 Hz. Traces are colored and sorted by the corresponding cell's phase at the stimulation frequency.[67] (h) Confocal imaging of a coronal section of the rat hippocampus expressing Lck-GCaMP6f following *in utero* electroporation.[91] (i) Mean calcium activity projection of a neuron expressing Lck-Gcamp6f following *in utero* electroporation and using 2P microscopy.[91] (j) Calcium traces from the same cortical neuron, with colors corresponding to the dashed ROIs in panel (i).[91]

used in mice, but several groups have applied these miniature microscopes in rats.[92,94–98,115] However, performance in these scopes is often optimized for mice. For example, early generations of UCLA microscopes have an FOV of ~1 mm^2. Next generation miniscopes designed with rats in mind have a larger FOV to account for the decreased cell density in the species (discussed in greater detail below).

The size and strength of the rat can create issues for the physical stability of head-mounted microscopes. Open-source systems, such as headcap covers, have been developed to protect and stabilize the scope.[116] A headcap system for protecting the microscope also permits a solution for reducing movement-related torque on the microscope from the tethering cable. Once implanted, an anchoring point on the headcap offset from the microscope can be used to fix the tether to the headcap and thus reduce force transferred at the connection point with the microscope.

4.5 Microprisms

As discussed, rat cortex is thicker relative to mouse cortex and this increased depth increases light scattering, decreases SNR, and prevents optical access to deep layers. One way to bypass these issues is to image through microprisms implanted directly into neural tissue as previously reported in mice.[117,118] Recently, Alexander et al.[92] successfully paired microprisms with head-mounted one-photon microscopes to image large populations of neurons in rat neocortex (Fig. 3). In this preparation, a 1 mm^2 microprism attached to a relay lens was positioned near neurons expressing GCaMP6f to create an FOV perpendicular to the dorsal surface of the brain spanning multiple cortical layers [Figs. 3(a)–3(c)]. A baseplate was attached to the skull above the microprism, which allowed a head-mounted microscope to be mounted [Fig. 3(d)]. Using this preparation, it was possible to simultaneously monitor calcium dynamics of hundreds of neurons with robust SNRs in Thy1-GCaMP6f transgenic rats performing track running or free exploration [Figs. 3(e)–3(k)]. Well known spatial coding properties of the retrosplenial cortex (RSC) were replicated using this method in rats including trajectory-dependent coding [Fig. 3(h)] and coding for environmental boundaries in egocentric coordinates [Fig. 3(k)].

4.6 Head-Mounted 1P Microscopes Designed for Rats

Head-mounted widefield microscopes with larger FOVs have been developed for rats (Fig. 4). Larger FOVs enable the monitoring of larger populations of neurons and permit the examination of cross-regional dynamics not afforded by a smaller FOV targeting a single brain region. Previously, researchers developed cScope, a head mounted widefield macroscope to access FOVs up to 8 mm^2 [Figs. 4(a)–4(c)].[37] cScope uses a hemodynamic illumination collar with green LEDs for reflectance illumination of cortical intrinsic signal and a blue LED for fluorescence imaging. Recordings using cScope have similar performance compared to conventional widefield epifluorescence microscopes, with imaging frame speed up to 30 Hz. However, the authors did not report cellular resolution calcium dynamics or whether this fluorescence signal originates from soma or neuropil.

A recent implementation of the UCLA Miniscope, Miniscope-LFOV, was developed for rats [Figs. 4(d)–4(f)].[36] This system is a one-photon microscope, which has two electrically adjustable working distance (± 100 μm) configurations that allow for cortical imaging via a cranial window and deep brain imaging via a relay GRIN lens. It has a 3.6 mm $\times$ 2.7 mm FOV, with one FOV in CA1 revealing 1357 cells.[36] The SNR in this microscope is considerably higher when compared with the performance of previous Miniscope iterations, attributable to newer and more sensitive detection systems in Miniscope-LFOV compared to its Miniscope predecessors. Recently published work details a system for online data pre-processing with Miniscope-LFOV,[119] enabling researchers to perform motion correction, calcium trace extraction, and recognize neural patterns, which are correlated to behavior.

4.7 Head-Mounted Multiphoton Microscopes Made for Rats

The carrying capacity of rats has facilitated the development of advanced head-mounted microscopes, such as multiphoton microscopes. The first head-mounted 2P microscope was developed for rats in the early 2000s, by Helmchen et al. [Figs. 5(a)–5(e)].[120] This microscope was 25 g in weight and 7.5 cm in height. Scanning was achieved by a fiber tip that resonated to form a Lissajous pattern. More recent iterations allow for increased performance, including raster scanning, and provide optical access to deeper areas with cellular resolution imaging in behaving rats [Figs. 5(f)–5(h)].[66] Today head mounted 3P microscopes for rats have cellular resolution as deep as 1.1 mm with a 150 μm square FOV [Figs. 5(i)–5(k)][38] and more recently adapted to mice.[121]

Like their tabletop counterparts, head-mounted multiphoton microscopes have several key features that facilitate calcium imaging *in vivo* in larger brained mammals, such as rats.

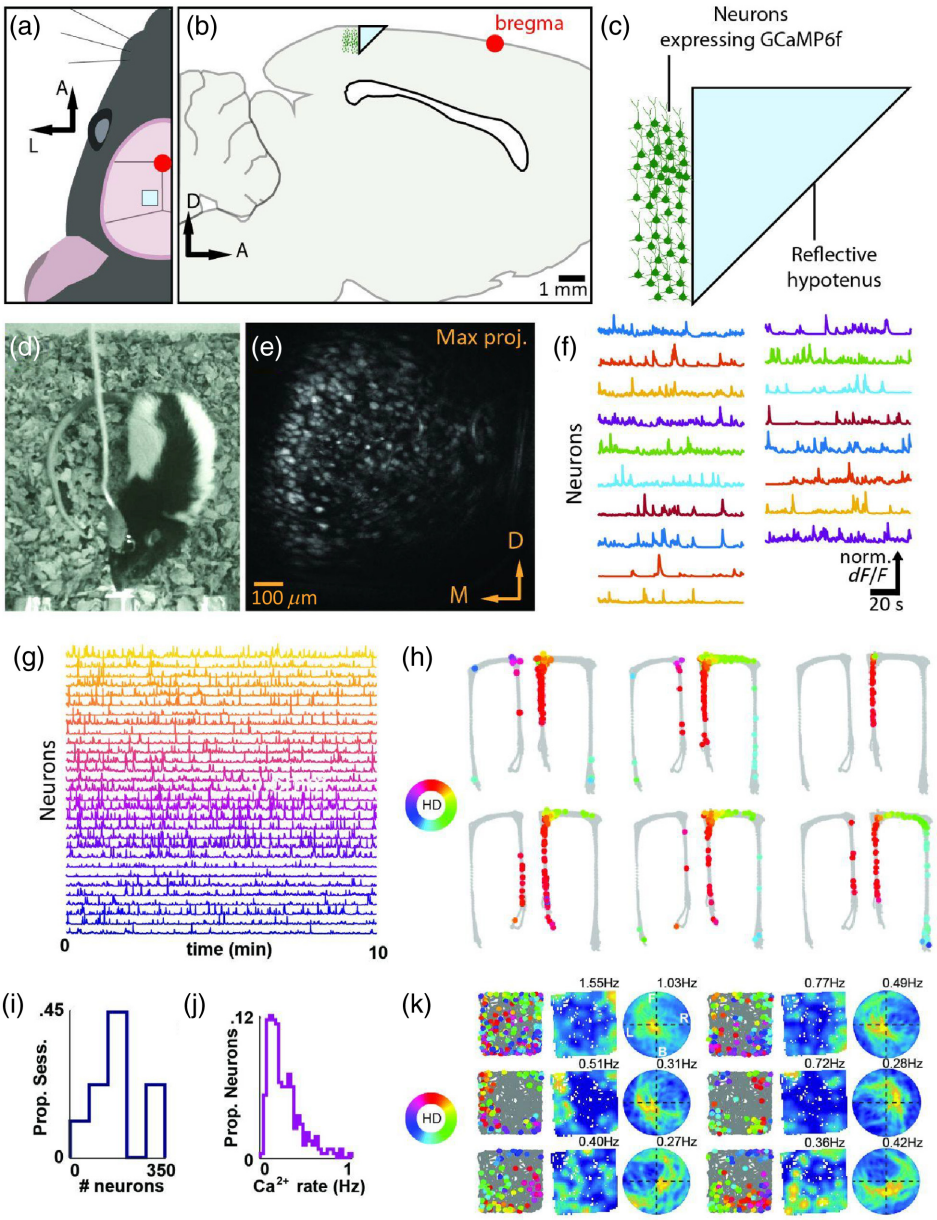

Fig. 3 Calcium imaging in transgenic rats through implanted microsprisms. (a) Position of the implanted microprism for imaging in the rat RSC relative to the rat head. (b) Schematic of the implantation location in a sagittal section. (c) Schematic of the prism imaging approach. (d) Image of an implanted rat wearing a head mounted one-photon camera in an operant chamber. (e) Maximum intensity projection from the imaging FOV. (f) Example time traces from selected ROIs from E showing fluorescence transients during an operant-based task. (g) Deconvolved Ca^{2+} traces from 30 simultaneously recorded RSC neurons. (h) Six RSC neurons, recorded using this preparation, exhibit differential activation for different trajectories on a delayed alternation spatial working memory task on a T-maze. Gray lines represent trajectory on track, split into leftward and rightward trials. Colored dots indicate animal position and head direction at the time of a calcium transient. Color indicates head direction according to legend on top right. (i) Number of cells per session. (j) Distribution of mean transient rate from a single recording. (k) Simultaneous recording of six RSC neurons with egocentric boundary vector responsivity. (Left) Trajectory plot with animal path in gray and spike locations indicated in colored circles where color is animal heading orientation in the environment. (Middle) Two-dimensional ratemap of "spiking" activity. (Right) Egocentric boundary ratemap showing position of boundaries at time of calcium transient. F, front; B, behind; R, right; L, left. All plots are maximum normalized (blue = zero activity, yellow = maximal).

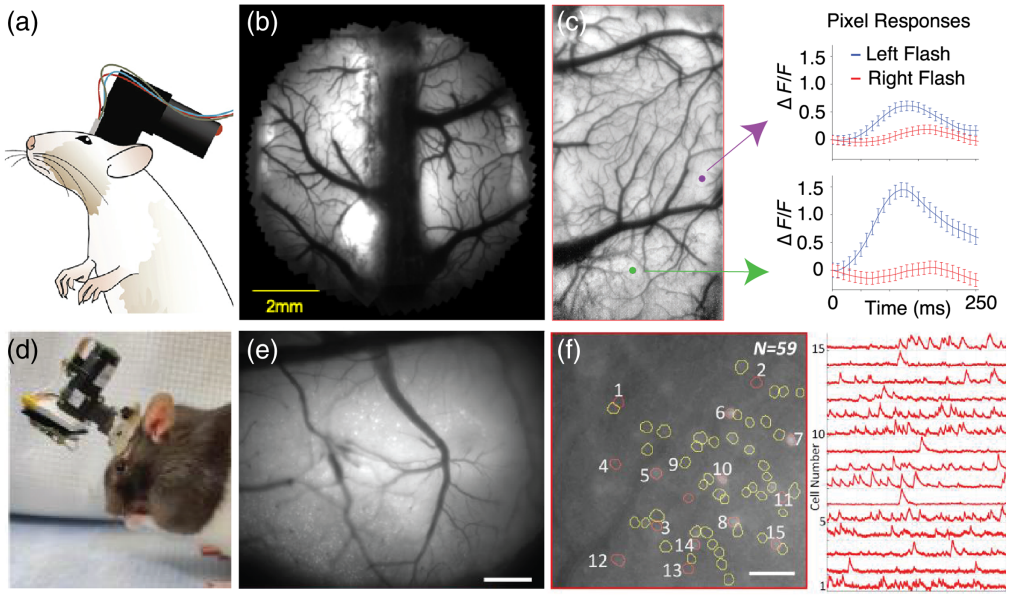

Fig. 4 Head mounted widefield microscopes designed for rats. (a) Schematic of a rat wearing cScope, a head-mounted widefield macroscope.[37] (b) Image of the FOV in a rat implanted with cScope. (c) Left: cScope fluorescence image, with colored dots indicating the location of the pixels that contribute to the responses on the right. Right: Flash response dynamics of the corresponding single pixel ROIs. (d) Picture of a rat wearing MiniLFOV.[36] (e) Maximum projection of a motion-corrected recording session. Scale bar: 500 μm. (f) Left: Map within panel (e) of 59 cells. Scale bar: 100 μm. Right: Calcium traces from a subset of 15 cells within panel (f) across 6 min.

The longer excitation wavelengths allow for less scattering in tissue and greater power delivery at depth. The non-linear properties of excitation provide optical sectioning and a reduction in out-of-focus excitation from fluorescence contamination from sources above and below the imaging plane.[13,122] Multiphoton imaging can improve the ability to resolve cellular structures like axonal projections and dendrites in scattering tissue and can reduce contamination from the neuropil *in vivo*.[123] However, head-mounted multiphoton microscopes are still outperformed by table top microscopes, including both commercial and custom systems, due to fewer space and weight constraints in the tabletop environment. Therefore, in order to combine the power to table top scopes with automated behavioral training systems, voluntary head restraint tools have been developed.

4.8 Voluntary Head-Restraint

Voluntary head-restraint is a system in which trained rodents submit to periods of mechanical head restraint for reward (Fig. 6). Initially developed for rats for repeatable presentation of visual stimuli,[61,62] demonstrations that computer controlled training systems for precise positioning and stability catalyzed renewed interest in voluntary head restraint.[63,126] Work in rats inspired researchers to develop automated behavioral systems using voluntary head-fixation in mice.[127–130] These head fixation systems have been designed for mechanical stability and repositioning within several microns and to be used together with widefield imaging or optogenetics.

Researchers have adapted voluntary restraint systems for cellular resolution population calcium imaging in behaving rats.[34,35,63] These systems used kinematic clamps to achieve high repositioning accuracy and produce the mechanical stability required by cellular resolution imaging [Figs. 6(d)–6(f)]. Kinematic clamps[131,132] are commonly used in optical and mechanical systems to achieve precise and repeatable alignment. To this end, recent work demonstrates that head fixation devices with micron-scale and submicron-scale repositioning accuracy for cellular resolution imaging are feasible.[124] These systems improved upon previously published Kelvin-style kinematic coupling systems[63] by utilizing a three vee-groove system, also known as a Maxwell system, which is simpler to manufacture and enables greater long-term performance.[133] The design principles described have been scaled up to evaluate voluntary head restraint in larger animals.[134]

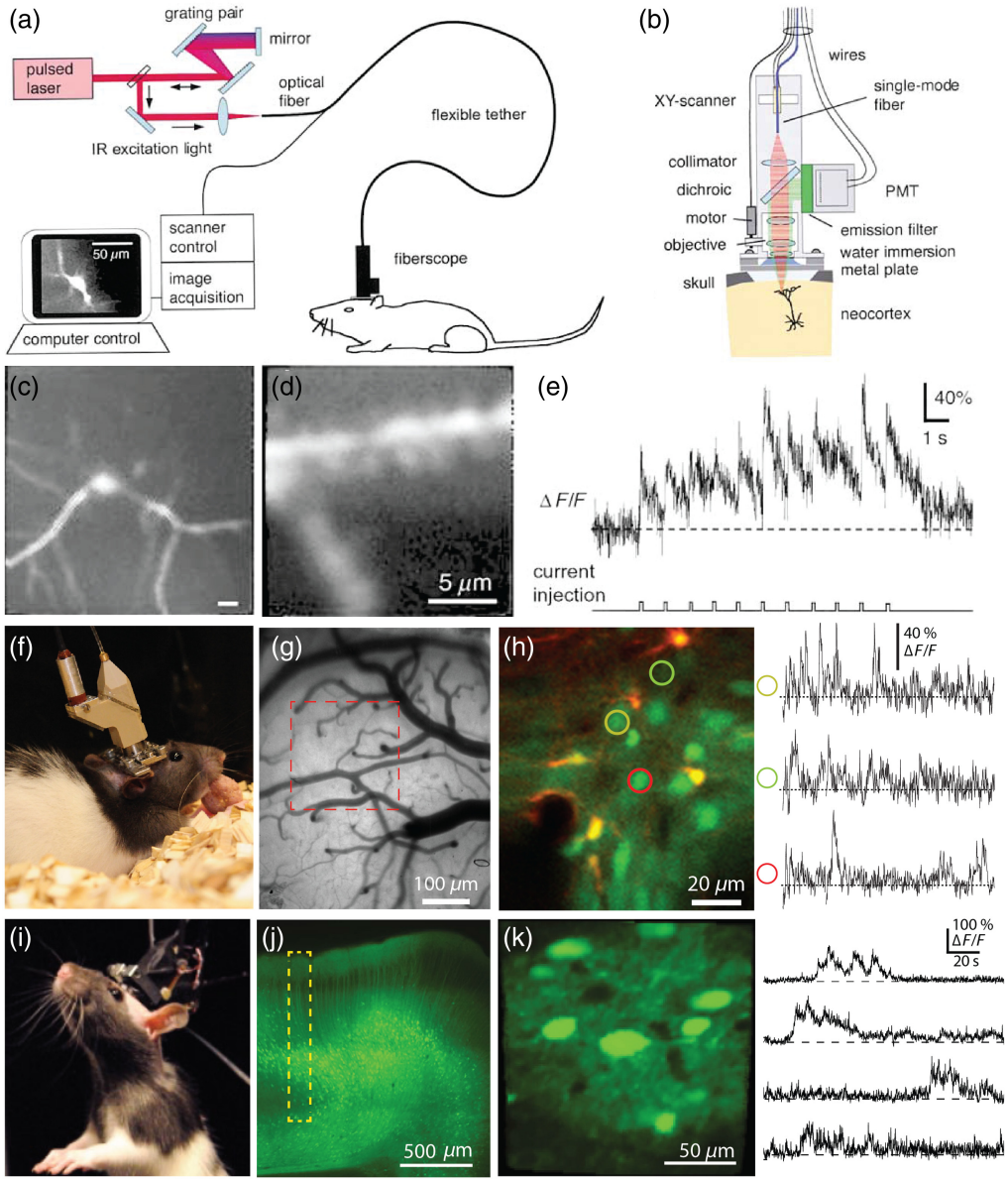

Fig. 5 Head-mounted multiphoton microscopes used in rats. (a) Diagram of the light path and setup of the first head-mounted 2P microscope.[120] (b) Schematic of the internal components in the fiberscope design. (c) Images of somatosensory cortex L2/3 neurons filled with calcium green-1. (d) Zoomed in image of a different dendrite from in somatosensory cortex L2/3. (e) Example calcium green-1 fluorescence trace along a dendritic process following current injection at 1 s intervals, with 10 ms resolution. (f) Picture of a rat wearing a head-mounted 2P microscope.[66] (g) Camera image of the primary visual area, with the 2P imaging sites identified with the red dashed line. (h) Left: Two color 2P imaging of primary visual cortex using sulforhodamine 101 and OGB1-AM. Right: calcium time courses of the soma of three neurons (colored circles in the left panel) across 30 s. (i) Image of a 120 g rat wearing a head mounted three-photon microscope.[38] (j) Histological section of GCaMP6s-labeled neurons in posterior parietal rat cortex, with the yellow dotted box showing the attainable imaging depth (1120 μm). (k) Left: Labeled neurons at 1120 μm depth below the cortical surface. Right: Example spontaneous calcium kinetics from FOV on left.

Recent work demonstrates the potential of combining voluntary head-restraint with transgenic rats to record neuron population dynamics over long timescales.[34] In this study, a new line of transgenic rats were reported to express GCaMP6f at high levels in hippocampal neurons. These rats were implanted with a newly developed magnetic-based kinematic coupling system and trained in voluntary restraint. Upon becoming proficient, animals performed hundreds of daily fixations over multiple months. 2P imaging through an implanted optical cannula over

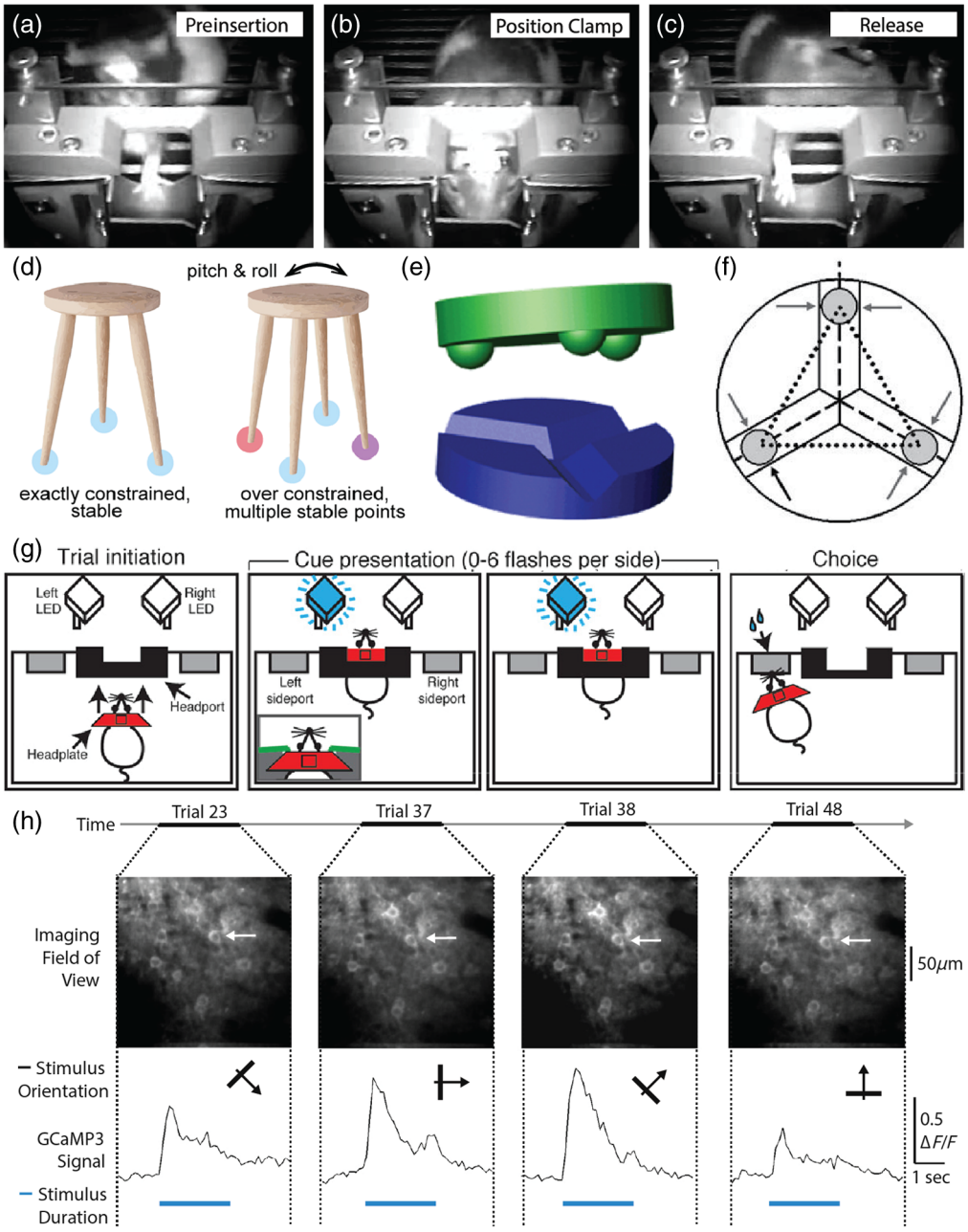

Fig. 6 Principles of voluntary head restraint. (a)–(c) A rat voluntarily head restraining across three stages: pre insertion, positioning of the head clamp and fixation, and release.[63] (d) The principles of kinematic coupling. Objects can be exactly constrained with stable points equal to the degrees of freedom the object has, or over-constrained such that there are multiple stable points possible. Kinematic coupling enables high degrees of repeatability and accuracy by exactly constraining objects.[124] (e) Toy model of a vee groove kinematic clamp.[124] (f) Diagram of the degrees of freedom constrained in a vee groove kinematic clamp.[125] (g) Behavioral paradigm schematic where rats are trained to voluntarily head restrain during an evidence accumulation task.[42] (h) 2P imaging of GCaMP3-labeled cortical neurons across several voluntary head-restraint trials. Top panels show V1 without motion correction. Bottom panel shows fluorescence transients from the selected neuron (indicated by the white arrow). On each trial, a visual stimulus was presented with differently oriented drifting gratings as denoted by the black arrow, with the blue line underneath indicating time of visual stimulus presentation.

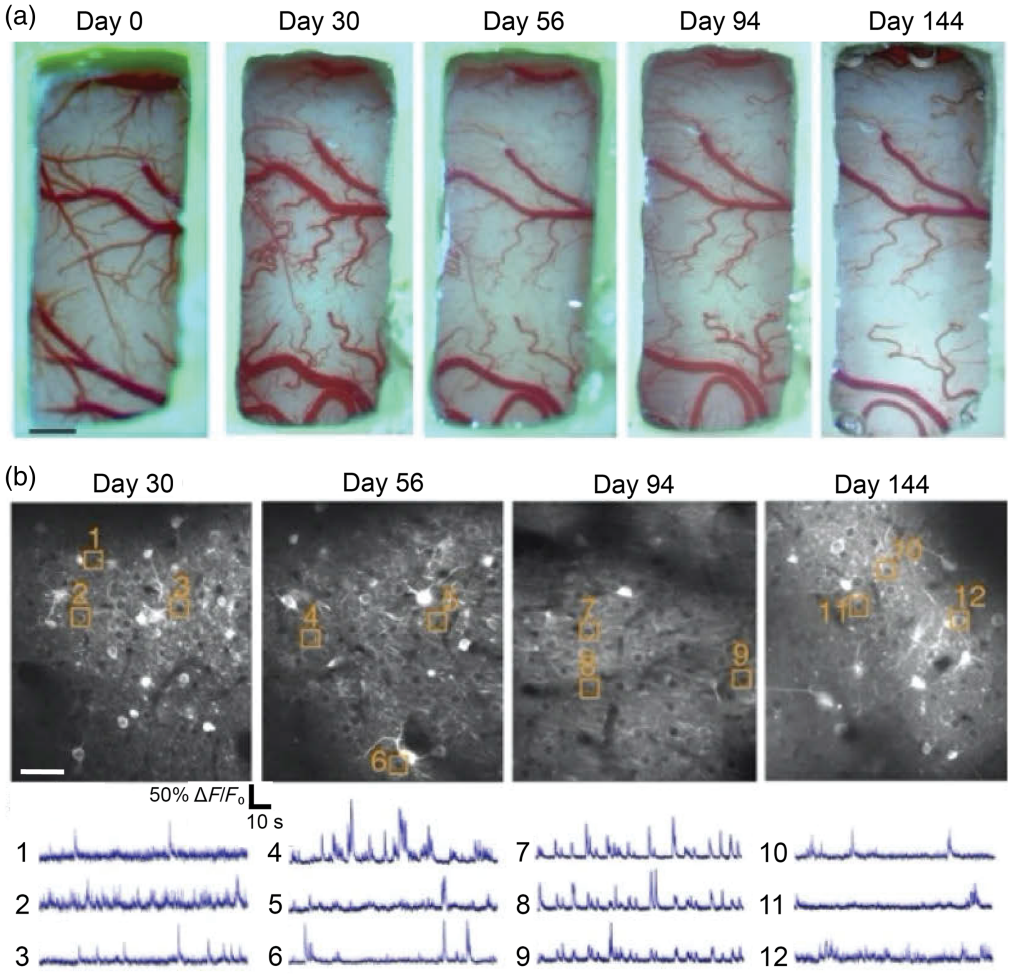

Fig. 7 Longitudinal 2P imaging in rats. (a) Brightfield images of the same cranial window in a rat, beginning from day of implantation (day 0). (b) 2P images of jGCaMP7s-expressing neurons with ROIs and the corresponding spontaneous activity traces from the somatosensory cortex of the same rat in (a). Note that the window quality remained high over 144 days, as reflected in the clarity of the window in the brightfield images.[93]

hippocampal CA1 provided the ability to track a large population of hippocampal neurons for well over a year. Other long term imaging preps (over 140 days) can also be achieved with viral labeling[93] (Fig. 7) and with fluorescent dextran (98 days).[135] We point out that each of these three groups removed the dura, and future studies will be required to evaluate the impact of different surgical preparations on longitudinal imaging in rats. These studies demonstrate the potential for longitudinal imaging in rats, which could be valuable for experiments on aging, plasticity, and representational drift.

5 Outlook

Below, we highlight future directions that may improve cellular resolution imaging in the rat model and may help experimentalists determine if the rat model is appropriate for their research program.

5.1 Next Generation Optical Design

Next generation imaging systems for rats may be improved by increasing the imaging depth, increasing the FOV of imaging systems, and enhancing the SNR to account for the physiological limitations discussed above. The use of 3P imaging can help compensate for the increase in cortical thickness and enable the recording of neuronal activity down to layer 5,[38] whereas the use of a large FOV instrument may compensate for the reduction in cell density. The combination

of the two, which has been recently described,[136,137] could enable activity recording from large neuronal populations in the rat.

Computational approaches have been used to reduce out-of-focus fluorescence neuropil contamination[123] and suppress measurement noise in calcium imaging data.[138,139] Aside from improving the quality of the data, reduction of noise and out-of-focus light can potentially enable deeper imaging in the rat brain. Computational methods may also aid with the development of new imaging systems. Software designed to simulate the optical, anatomical, and physiological properties of the mouse brain[140] may allow for rapid development of next generation imaging systems and provide a standardized ground truth for evaluating their performance. Extending this simulation tool to rats would be a valuable next step and should be feasible given the extensive physiological data available.[69,70,80,81]

5.2 Imaging in Cellular Compartments

Several new molecular genetic approaches could be considered in order to improve imaging performance in rats. For example, neuropil contamination could be reduced by expression of soma restricted calcium sensors.[141,142] In addition, simultaneous imaging of multiple cell types could be achieved by restricting sensors to readily differentiable cellular compartments, such as axons and soma. Finally, imaging of apical dendrites could allow access to deep cortical neurons, an approach used to support population imaging in macaques.[143]

5.3 Multi-Device Imaging

The larger size of the rat loosens spatial constraints with neuroimaging methods. One way would be to incorporate multiple head-mounted microscopes targeting different regions, akin to *in vivo* electrophysiology. This approach has been applied in mice by targeting two distant regions of interest (ROIs) by developing a smaller one-photon microscope configuration.[144,145] Multiple off-the-shelf head-mounted microscopes could be situated on the rat skull using angled, longer relay lenses; this would enable proper clearance for the microscope and lens attachment.

A similar method could be utilized to pair *in vivo* neuroimaging, *in vivo* electrophysiology, or perturbation methods in freely behaving rats. As a consequence of a greater working area, ferrules or cannulae could be positioned in areas outside of the imaging window, counter to current methods that record calcium dynamics and provide optogenetic stimulation within the same FOV. Calcium activity of large neural ensembles or neuromodulatory dynamics in one region could be compared with respect to electrophysiological activity—including oscillatory dynamics—in another area.[115] Neuroimaging signals in the same FOV could be compared before and after optogenetic or pharmacological manipulations to another structure.

6 Conclusion

Extending neuroscience tools to a diverse set of species will allow researchers to study how the brains of different species solve similar biological problems.[146] This is synergistic with new priorities for cross-species comparative work, in which similar behavioral methods and recording tools are applied across multiple species.[147–149] Expanding technologies to organisms beyond the species that the technology was originally developed poses a significant challenge. It is our hope that rats can serve both as a valuable model for systems neuroscience and act as a bridge to new framework for applying *in vivo* imaging tools more broadly across a diverse set of species.

Disclosures

No conflicts of interest, financial or otherwise, are declared by the authors.

Code and Data Availability

Data sharing is not applicable to this article, as no new data were created or analyzed.

Author Contributions

SJK and ASA drafted the manuscript with support from HF, BBS, and ROA. All authors contributed to the editing of the manuscript.

Acknowledgments

SJK is supported by an award from the National Institute on Deafness and Other Communication Disorders (TC32 DC000023). ROA is supported by an award from the National Institutes of Health (NIH Blueprint DSPAN F99NS130925). BBS is supported by NIH award R56MH132732 and a Whitehall Foundation research grant. ASA is supported by NIH award K99 NS119665. We thank Jerry Chen, Jack Giblin, and Aneesh Bal for comments on the manuscript.

References

1. Y. Zhang et al., "Fast and sensitive GCaMP calcium indicators for imaging neural populations," *Nature* **615**, 884–891 (2023).
2. M. Kannan et al., "Dual-polarity voltage imaging of the concurrent dynamics of multiple neuron types," *Science* **378**(6619), eabm8797 (2022).
3. T. Patriarchi et al., "Ultrafast neuronal imaging of dopamine dynamics with designed genetically encoded sensors," *Science* **360**(6396), eaat4422 (2018).
4. T. Patriarchi et al., "An expanded palette of dopamine sensors for multiplex imaging *in vivo*," *Nat. Methods* **17**(11), 1147–1155 (2020).
5. N. J. Sofroniew et al., "A large field of view two-photon mesoscope with subcellular resolution for in vivo imaging," *eLife* **5**, e14472 (2016).
6. C. H. Yu et al., "Diesel2p mesoscope with dual independent scan engines for flexible capture of dynamics in distributed neural circuitry," *Nat. Commun.* **12**(1), 6639 (2021).
7. W. Zong et al., "Large-scale two-photon calcium imaging in freely moving mice," *Cell* **185**(7), 1240–1256.e30 (2022).
8. J. P. Cunningham and B. M. Yu, "Dimensionality reduction for large-scale neural recordings," *Nat. Neurosci.* **17**(11), 1500–1509 (2014).
9. I. H. Stevenson and K. P. Kording, "How advances in neural recording affect data analysis," *Nat. Neurosci.* **14**(2), 139–142 (2011).
10. A. E. Urai et al., "Large-scale neural recordings call for new insights to link brain and behavior," *Nat. Neurosci.* **25**(1), 11–19 (2022).
11. C. Grienberger and A. Konnerth, "Imaging calcium in neurons," *Neuron* **73**(5), 862–885 (2012).
12. G. Grynkiewicz, M. Poenie, and R. Y. Tsien, "A new generation of Ca^{2+} indicators with greatly improved fluorescence properties," *J. Biol. Chem.* **260**(6), 3440–3450 (1985).
13. W. Denk, J. H. Strickler, and W. W. Webb, "Two-photon laser scanning fluorescence microscopy," *Science* **248**(4951), 73–76 (1990).
14. A. Miyawaki et al., "Fluorescent indicators for Ca^{2+} based on green fluorescent proteins and calmodulin," *Nature* **388**(6645), 882–887 (1997).
15. D. A. Dombeck et al., "Imaging large-scale neural activity with cellular resolution in awake, mobile mice," *Neuron* **56**(1), 43–57 (2007).
16. D. A. Dombeck et al., "Functional imaging of hippocampal place cells at cellular resolution during virtual navigation," *Nat. Neurosci.* **13**(11), 1433–1440 (2010).
17. K. K. Ghosh et al., "Miniaturized integration of a fluorescence microscope," *Nat. Methods* **8**(10), 871–878 (2011).
18. T. W. Chen et al., "Ultrasensitive fluorescent proteins for imaging neuronal activity," *Nature* **499**(7458), 295–300 (2013).
19. D. J. Cai et al., "A shared neural ensemble links distinct contextual memories encoded close in time," *Nature* **534**(7605), 115–118 (2016).
20. A. Fassihi et al., "Tactile perception and working memory in rats and humans," *Proc. Natl. Acad. Sci. U. S. A.* **111**(6), 2331–2336 (2014).
21. A. S. Reinhold et al., "Behavioral and neural correlates of hide-and-seek in rats," *Science* **365**(6458), 1180–1183 (2019).
22. R. Poddar, R. Kawai, and B. P. Ölveczky, "A fully automated high-throughput training system for rodents," *PLoS One* **8**(12), e83171 (2013).
23. L. Madisen et al., "Transgenic mice for intersectional targeting of neural sensors and effectors with high specificity and performance," *Neuron* **85**(5), 942–958 (2015).
24. N. El-Ayache and J. J. Galligan, "The rat in neuroscience research," in *The Laboratory Rat*, M. A. Suckow et al., Eds., pp. 1003–1022, Academic Press (2020).
25. S. A. Barnett, *The Story of Rats: Their Impact on Us and Our Impact on Them*, Allen and Unwin (2002).
26. J. Altman and G. D. Das, "Autoradiographic and histological evidence of postnatal hippocampal neurogenesis in rats," *J. Comp. Neurol.* **124**(3), 319–335 (1965).
27. J. O'Keefe and J. Dostrovsky, "The hippocampus as a spatial map: preliminary evidence from unit activity in the freely-moving rat," *Brain Res.* **34**, 171–175 (1971).

28. J. S. Taube, R. U. Muller, and J. B. Ranck, "Head-direction cells recorded from the postsubiculum in freely moving rats. I. Description and quantitative analysis," *J. Neurosci.* **10**(2), 420–435 (1990).
29. S. Ogawa et al., "Brain magnetic resonance imaging with contrast dependent on blood oxygenation," *Proc. Natl. Acad. Sci. U. S. A.* **87**(24), 9868–9872 (1990).
30. L. Buck and R. Axel, "A novel multigene family may encode odorant receptors: a molecular basis for odor recognition," *Cell* **65**(1), 175–187 (1991).
31. M. A. Wilson and B. L. McNaughton, "Reactivation of hippocampal ensemble memories during sleep," *Science* **265**(5172), 676–679 (1994).
32. W. Denk et al., "Anatomical and functional imaging of neurons using 2-photon laser scanning microscopy," *J. Neurosci. Methods* **54**(2), 151–162 (1994).
33. T. Hafting et al., "Microstructure of a spatial map in the entorhinal cortex," *Nature* **436**(7052), 801–806 (2005).
34. P. D. Rich et al., "Magnetic voluntary head-fixation in transgenic rats enables lifetime imaging of hippocampal neurons," bioRxiv, 2023-08 (2023).
35. B. B. Scott et al., "Fronto-parietal cortical circuits encode accumulated evidence with a diversity of timescales," *Neuron* **95**(2), 385–398.e5 (2017).
36. C. Guo et al., "Miniscope-LFOV: a large field of view, single cell resolution, miniature microscope for wired and wire-free imaging of neural dynamics in freely behaving animals," *Sci. Adv.* **9**, eadg3918 (2023).
37. B. B. Scott et al., "Imaging cortical dynamics in GCaMP transgenic rats with a head-mounted widefield macroscope," *Neuron* **100**(5), 1045–1058.e5 (2018).
38. A. Klioutchnikov et al., "Three-photon head-mounted microscope for imaging deep cortical layers in freely moving rats," *Nat. Methods* **17**(5), 509–513 (2020).
39. B. W. Brunton, M. M. Botvinick, and C. D. Brody, "Rats and humans can optimally accumulate evidence for decision-making," *Science* **340**(6128), 95–98 (2013).
40. C. M. Constantinople, A. T. Piet, and C. D. Brody, "An analysis of decision under risk in rats," *Curr. Biol.* **29**(12), 2066–2074.e5 (2019).
41. A. Kepecs et al., "Neural correlates, computation and behavioural impact of decision confidence," *Nature* **455**(7210), 227–231 (2008).
42. B. B. Scott et al., "Sources of noise during accumulation of evidence in unrestrained and voluntarily head-restrained rats," *eLife* **4**, e11308 (2015).
43. N. Uchida, A. Kepecs, and Z. F. Mainen, "Seeing at a glance, smelling in a whiff: rapid forms of perceptual decision making," *Nat. Rev. Neurosci.* **7**(6), 485–491 (2006).
44. A. Akrami et al., "Posterior parietal cortex represents sensory history and mediates its effects on behavior," *Nature* **554** (7692), 368–372 (2018).
45. K. J. Miller, M. M. Botvinick, and C. D. Brody, "Dorsal hippocampus contributes to model-based planning," *Nat. Neurosci.* **20**(9), 1269–1276 (2017).
46. K. J. Miller, M. M. Botvinick, and C. D. Brody, "Value representations in the rodent orbitofrontal cortex drive learning, not choice," *eLife* **11**, e64575 (2022a).
47. T. S. Critchfield, "Translational contributions of the experimental analysis of behavior," *Behav. Anal.* **34**, 3–17 (2011).
48. J. W. Young and A. Markou, "Translational rodent paradigms to investigate neuromechanisms underlying behaviors relevant to amotivation and altered reward processing in schizophrenia," *Schizophr. Bull.* **41**(5), 1024–1034 (2015).
49. E. G. Patterson-Kane, M. Hunt, and D. Harper, "Rats demand social contact," *Anim. Welfare* **11**(3), 327–332 (2002).
50. C. Rutte and M. Taborsky, "Generalized reciprocity in rats," *PLoS Biol.* **5**(7), e196 (2007).
51. D. S. Viana et al., "Cognitive and motivational requirements for the emergence of cooperation in a rat social game," *PLoS One* **5**(1), e8483 (2010).
52. I. B. A. Bartal, J. Decety, and P. Mason, "Empathy and pro-social behavior in rats," *Science* **334**(6061), 1427–1430 (2011).
53. M. Nagy et al., "Synergistic benefits of group search in rats," *Curr. Biol.* **30**, 4733–4738.e4 (2020).
54. V. Pedrosa et al., "Humans, rats and mice show species-specific adaptations to sensory statistics in categorisation behavior," bioRxiv, 2023-01 (2023).
55. I. Q. Whishaw et al., "Accelerated nervous system development contributes to behavioral efficiency in the laboratory mouse: a behavioral review and theoretical proposal," *Dev. Psychobiol.* **39**(3), 151–170 (2001).
56. V. Vengeliene, A. Bilbao, and R. Spanagel, "The alcohol deprivation effect model for studying relapse behavior: a comparison between rats and mice," *Alcohol* **48**(3), 313–320 (2014).
57. D. Aronov and D. W. Tank, "Engagement of neural circuits underlying 2D spatial navigation in a rodent virtual reality system," *Neuron* **84**(2), 442–456 (2014).
58. C. Holscher et al., "Rats are able to navigate in virtual environments," *J. Exp. Biol.* **208**(3), 561–569 (2005).
59. K. Safaryan and M. R. Mehta, "Enhanced hippocampal theta rhythmicity and emergence of eta oscillation in virtual reality," *Nat. Neurosci.* **24**(8), 1065–1070 (2021).

60. T. J. Bussey et al., "The touchscreen cognitive testing method for rodents: how to get the best out of your rat," *Learn. Mem.* **15**(7), 516–523 (2008).
61. S. V. Girman, "Means of restricting the movements of conscious rats in neurophysiologic experiments," *Zh. Vyssh. Nerv. Deiat. Im. IP Pavlova* **30**(5), 1087–1089 (1980).
62. S. V. Girman, "Responses of neurons of primary visual cortex of awake unrestrained rats to visual stimuli," *Neurosci. Behav. Physiol.* **15**, 379–386 (1985).
63. B. B. Scott, C. D. Brody, and D. W. Tank, "Cellular resolution functional imaging in behaving rats using voluntary head restraint," *Neuron* **80**(2), 371–384 (2013).
64. K. Luxem et al., "Open-source tools for behavioral video analysis: setup, methods, and best practices," *eLife* **12**, e79305 (2023).
65. Charles River Laboratories, Long Evans Rat, https://www.criver.com/products-services/find-model/long-evans-rat (accessed 19 November 2023).
66. J. Sawinski et al., "Visually evoked activity in cortical cells imaged in freely moving animals," *Proc. Natl. Acad. Sci. U. S. A.* **106**(46), 19557–19562 (2009).
67. J. Y. Rhee et al., "Neural correlates of visual object recognition in rats," (2023).
68. C. Schwarz et al., "The head-fixed behaving rat—procedures and pitfalls," *Somatosens. Mot. Res.* **27**(4), 131–148 (2010).
69. S. Herculano-Houzel, B. Mota, and R. Lent, "Cellular scaling rules for rodent brains," *Proc. Natl. Acad. Sci. U. S. A.* **103**(32), 12138–12143 (2006).
70. S. Herculano-Houzel et al., "Mammalian brains are made of these: a dataset of the numbers and densities of neuronal and nonneuronal cells in the brain of glires, primates, scandentia, eulipotyphlans, afrotherians and artiodactyls, and their relationship with body mass," *Brain Behav. Evol.* **86**(3–4), 145–163 (2015).
71. A. J. Rockel, R. W. Hiorns, and T. P. Powell, "The basic uniformity in structure of the neocortex," *Brain* **103**(2), 221–244 (1980).
72. C. Beaulieu, "Numerical data on neocortical neurons in adult rat, with special reference to the GABA population," *Brain Res.* **609**(1–2), 284–292 (1993).
73. A. Morales-Gregorio, A. van Meegen, and S. J. van Albada, "Ubiquitous lognormal distribution of neuron densities in mammalian cerebral cortex," *Cerebral Cortex* **33**(16), 9439–9449 (2023).
74. M. Azimipour et al., "Extraction of optical properties and prediction of light distribution in rat brain tissue," *J. Biomed. Opt.* **19**(7), 075001 (2014).
75. D. Kleinfeld and W. Denk, *Two-Photon Imaging of Cortical Microcirculation. Imaging in Neuroscience and Development: A Laboratory Manual*, pp. 701–705, Cold Spring Harbor Laboratory Press, Cold Spring Harbor (2000).
76. M. Oheim et al., "Two-photon microscopy in brain tissue: parameters influencing the imaging depth," *J. Neurosci. Methods* **111**(1), 29–37 (2001).
77. D. Kobat et al., "Deep tissue multiphoton microscopy using longer wavelength excitation," *Opt. Express* **17**(16), 13354–13364 (2009).
78. T. Wang et al., "Quantitative analysis of 1300-nm three-photon calcium imaging in the mouse brain," *eLife* **9**, e53205 (2020).
79. K. Svoboda et al., "Spread of dendritic excitation in layer 2/3 pyramidal neurons in rat barrel cortex *in vivo*," *Nat. Neurosci.* **2**(1), 65–73 (1999).
80. P. Blinder et al., "The cortical angiome: an interconnected vascular network with noncolumnar patterns of blood flow," *Nat. Neurosci.* **16**(7), 889–897 (2013).
81. P.S. Tsai et al., "Correlations of neuronal and microvascular densities in murine cortex revealed by direct counting and colocalization of nuclei and vessels," *J. Neurosci.* **29**(46), 14553–14570 (2009).
82. V. V. Barun and A. P. Ivanov, "Estimate of the contribution of localized light absorption by blood vessels to the optical properties of biological tissue," *Opt. Spectrosc.* **96**, 940–945 (2004).
83. E. Chaigneau et al., "Two-photon imaging of capillary blood flow in olfactory bulb glomeruli," *Proc. Natl. Acad. Sci. U. S. A.* **100**, 13081–13086 (2003).
84. D. Wang et al., "Biocompatible and photostable AIE dots with red emission for in vivo two-photon bio-imaging," *Sci. Rep.* **4**(1), 4279 (2014).
85. M. Vedi et al., "2022 updates to the rat genome database: a findable, accessible, interoperable, and reuslable (FAIR) resource," *Genetics* **224**, iyad042 (2023).
86. J. R. Pettibone et al., "Knock-in rat lines with cre recombinase at the dopamine D1 and adenosine 2a receptor loci," *eNeuro* **6**(5), ENEURO.0163-19.2019 (2019).
87. G. D. Stuber, A. M. Stamatakis, and P. A. Kantak, "Considerations when using cre-driver rodent lines for studying ventral tegmental area circuitry," *Neuron* **85**(2), 439–445 (2015).
88. I. B. Witten et al., "Recombinase-driver rat lines: tools, techniques, and optogenetic application to dopamine-mediated reinforcement," *Neuron* **72**(5), 721–733 (2011).
89. Simons Foundation, "Simons Foundation Autism Research Initiative (SFARI) rat models," https://www.sfari.org/resource/rat-models/ (2022).

90. Rat Genome Database, https://rgd.mcw.edu/wg/resource-links/#rat_resources (accessed 19 November 2023).
91. J. M. Gee et al., "Imaging activity in astrocytes and neurons with genetically encoded calcium indicators following *in utero* electroporation," *Front. Mol. Neurosci.* **8**, 10 (2015).
92. A. S. Alexander, B. B. Scott, and M. E. Hasselmo, "Laminar and projection-specific calcium imaging of spatial memory related retrosplenial cortex dynamics in freely moving rats," in *Prog. No 866.05. Neurosci. Meeting Planner*, Society for Neuroscience (2021).
93. S. Chornyy et al., "Cellular-resolution monitoring of ischemic stroke pathologies in the rat cortex," *Biomed. Opt. Express* **12**(8), 4901–4919 (2021).
94. C. M. Cameron et al., "Increased cocaine motivation is associated with degraded spatial and temporal representations in IL-NAc neurons," *Neuron* **103**(1), 80–91.e7 (2019).
95. F. Gobbo et al., "Neuronal signature of spatial decision-making during navigation by freely moving rats by using calcium imaging," *Proc. Natl. Acad. Sci. U. S. A.* **119**(44), e2212152119 (2022).
96. E. E. Hart et al., "Chemogenetic modulation and single-photon calcium imaging in anterior cingulate cortex reveal a mechanism for effort-based decisions," *J. Neurosci.* **40**(29), 5628–5643 (2020).
97. H. S. Wirtshafter and J. F. Disterhoft, "*In vivo* multi-day calcium imaging of CA1 hippocampus in freely moving rats reveals a high preponderance of place cells with consistent place fields," *J. Neurosci.* **42**(22), 4538–4554 (2022).
98. H. S. Wirtshafter and J. F. Disterhoft, "Place cells are nonrandomly clustered by field location in CA1 hippocampus," *Hippocampus* **33**(2), 65–84 (2023).
99. T. L. Daigle et al., "A suite of transgenic driver and reporter mouse lines with enhanced brain-cell-type targeting and functionality," *Cell* **174**(2), 465–480.e22 (2018).
100. H. K. Decot et al., "Coordination of brain-wide activity dynamics by dopaminergic neurons," *Neuropsychopharmacology* **42**(3), 615–627 (2017).
101. R. C. Challis et al., "Systemic AAV vectors for widespread and targeted gene delivery in rodents," *Nat. Protoc.* **14**(2), 379–414 (2019).
102. R. D. Dayton, M. S. Grames, and R. L. Klein, "More expansive gene transfer to the rat CNS: AAV PHP. EB vector dose–response and comparison to AAV PHP.B," *Gene Ther.* **25**(5), 392–400 (2018).
103. K. L. Jackson, R. D. Dayton, and R. L. Klein, "AAV9 supports wide-scale transduction of the CNS and TDP-43 disease modeling in adult rats," *Mol. Ther. Methods Clin. Dev.* **2**, 15036 (2015).
104. D. Chatterjee et al., "Enhanced CNS transduction from AAV. PHP. eB infusion into the cisterna magna of older adult rats compared to AAV9," *Gene Ther.* **29**(6), 390–397 (2022).
105. K. L. Pietersz et al., "Transduction patterns in the CNS following various routes of AAV-5-mediated gene delivery," *Gene Ther.* **28**(7–8), 435–446 (2021).
106. K. L. Jackson et al., "Better targeting, better efficiency for wide-scale neuronal transduction with the synapsin promoter and AAV-PHP.B," *Front. Mol. Neurosci.* **9**, 116 (2016).
107. D. J. Garrett et al., "*In utero* recombinant adeno-associated virus gene transfer in mice, rats, and primates," *BMC Biotech.* **3**, 16 (2003).
108. T. Saito and N. Nakatsuji, "Efficient gene transfer into the embryonic mouse brain using in vivo electroporation," *Dev. Biol.* **240**(1), 237–246 (2001).
109. J. Szczurkowska et al., "Targeted *in vivo* genetic manipulation of the mouse or rat brain by *in utero* electroporation with a triple-electrode probe," *Nat. Protoc.* **11**, 399–412 (2016).
110. H. Tabata and K. Nakajima, "Efficient *in utero* gene transfer system to the developing mouse brain using electroporation: visualization of neuronal migration in the developing cortex," *Neuroscience* **103**(4), 865–872 (2001).
111. W. Walantus, L. Elias, and A. Kriegstein, "*In utero* intraventricular injection and electroporation of E16 rat embryos," *J. Vis. Exp.* (6), e236 (2007).
112. L. Chansel-Debordeaux et al., "*In utero* delivery of rAAV2/9 induces neuronal expression of the transgene in the brain: towards new models of Parkinson's disease," *Gene Ther.* **24**(12), 801–809 (2017).
113. J. M. Rosin and D. M. Kurrasch, "*In utero* electroporation induces cell death and alters embryonic microglia morphology and expression signatures in the developing hypothalamus," *J. Neuroinflammation* **15**(1), 181 (2018).
114. D. Aharoni and T. M. Hoogland, "Circuit investigations with open-source miniaturized microscopes: past, present and future," *Front. Cell Neurosci.* **13**, 141 (2019).
115. N. R. Kinsky, J. Haddad, and K. Diba, "Combined electrophysiology and imaging to investigate hippocampal-cortical interactions during memory consolidation," in *Soc. Neurosci. Abstr.* (2022).
116. K. Saxena et al., "iHELMET: a 3D-printing solution for safe endoscopic Ca^{2+} recording in social neuroscience," *J. Neurosci. Methods* **355**, 109109 (2021).
117. M. L. Andermann et al., "Chronic cellular imaging of entire cortical columns in awake mice using microprisms," *Neuron* **80**(4), 900–913 (2013).

118. S. Gulati, V. Y. Cao, and S. Otte, "Multi-layer cortical Ca^{2+} imaging in freely moving mice with prism probes and miniaturized fluorescence microscopy," *J. Vis. Exp.* **124**, e55579 (2017).
119. Z. Chen et al., "A hardware system for real-time decoding of *in vivo* calcium imaging data," *eLife* **12**, e78344 (2023).
120. F. Helmchen et al., "A miniature head-mounted two-photon microscope: high-resolution brain imaging in freely moving animals," *Neuron* **31**(6), 903–912 (2001).
121. A. Klioutchnikov et al., "A three-photon head-mounted microscope for imaging all layers of visual cortex in freely moving mice," *Nat. Methods* **20**, 610–616 (2022).
122. F. Helmchen and W. Denk, "Deep tissue two-photon microscopy," *Nat. Methods* **2**(12), 932–940 (2005).
123. A. Glas et al., "Benchmarking miniaturized microscopy against two-photon calcium imaging using single-cell orientation tuning in mouse visual cortex," *PLoS One* **14**(4), e0214954 (2019).
124. S. J. Kim, A. H. Slocum, and B. B. Scott, "A miniature kinematic coupling device for mouse head fixation," *J. Neurosci. Methods* **372**, 109549 (2022).
125. M. L. Culpepper, "Design of quasi-kinematic couplings," *Precis. Eng.* **28**(3), 338–357 (2004).
126. A. R. Kampff et al., "The voluntary head-restrained rat," in *Program No. 819.18. 2010 Neurosci. Meeting Planner*, Society for Neuroscience, San Diego, California (2010)
127. R. Aoki et al., "An automated platform for high-throughput mouse behavior and physiology with voluntary head-fixation," *Nat. Commun.* **8**(1), 1196 (2017).
128. Y. Hao, A. M. Thomas, and N. Li, "Fully autonomous mouse behavioral and optogenetic experiments in home-cage," *eLife* **10**, e66112 (2021).
129. T. H. Murphy et al., "High-throughput automated home-cage mesoscopic functional imaging of mouse cortex," *Nat. Commun.* **7**(1), 11611 (2016).
130. T. H. Murphy et al., "Automated task training and longitudinal monitoring of mouse mesoscale cortical circuits using home cages," *eLife* **9**, e55964 (2020).
131. C. Evans, *Precision Engineering: An Evolutionary View*, Cranfield Press, Bedford (1989).
132. J. C. Maxwell and W. D. Niven, "General considerations concerning scientific apparatus," *Sci. Pap. JC Maxwell* **2**, 507–508 (1890).
133. A. H. Slocum, "Design of three-groove kinematic couplings," *Precis. Eng.* **14**(2), 67–76 (1992).
134. J. D. Walker et al., "A platform for semiautomated voluntary training of common marmosets for behavioral neuroscience," *J. Neurophysiol.* **123**(4), 1420–1426 (2020).
135. M. M. Koletar et al., "Refinement of a chronic cranial window implant in the rat for longitudinal *in vivo* two-photon fluorescence microscopy of neurovascular function," *Sci. Rep.* **9**(1), 5499 (2019).
136. A. T. Mok et al., "A large field of view two-and three-photon microscope for high-resolution deep tissue imaging," in *CLEO: Appl. and Technol.*, Optica Publishing Group, p. ATh5A-1 (2023).
137. N. R. Shvedov et al., "Deep brain three-photon imaging in transgenic songbirds," in *Program No. PSTR090.14. 2023 Neurosci. Meeting Planner*, Society for Neuroscience, Washington DC, Online (2023).
138. X. Li et al., "Reinforcing neuron extraction and spike inference in calcium imaging using deep self-supervised denoising," *Nat. Methods* **18**(11), 1395–1400 (2021).
139. J. Platisa et al., "High-speed low-light *in vivo* two-photon voltage imaging of large neuronal populations," *Nat. Methods* **20**, 1095–1103 (2023).
140. A. Song et al., "Neural anatomy and optical microscopy (NAOMi) simulation for evaluating calcium imaging methods," *J. Neurosci. Methods* **358**, 109173 (2021).
141. Y. Chen et al., "Soma-targeted imaging of neural circuits by ribosome tethering," *Neuron* **107**(3), 454–469.e6 (2020).
142. S. Grødem et al., "An updated suite of viral vectors for *in vivo* calcium imaging using intracerebral and retro-orbital injections in male mice," *Nat. Commun.* **14**(1), 608 (2023).
143. E. M. Trautmann et al., "Dendritic calcium signals in rhesus macaque motor cortex drive an optical brain-computer interface," *Nat. Commun.* **12**(1), 3689 (2021).
144. A. de Groot et al., "NINscope, a versatile miniscope for multi-region circuit investigations," *eLife* **9**, e49987 (2020).
145. W. G. Gonzalez et al., "Persistence of neuronal representations through time and damage in the hippocampus," *Science* **365**(6455), 821–825 (2019).
146. G. Laurent, "On the value of model diversity in neuroscience," *Nat. Rev. Neurosci.* **21**(8), 395–396 (2020).
147. D. Badre, M. J. Frank, and C. I. Moore, "Interactionist neuroscience," *Neuron* **88**, 855–860 (2015).
148. H. C. Barron et al., "Cross-species neuroscience: closing the explanatory gap," *Philos. Trans. R. Soc. B Biol. Sci.* **376**, 20190633 (2021).
149. M. M. Nour, Y. Liu, and R. J. Dolan, "Functional neuroimaging in psychiatry and the case for failing better," *Neuron* **110**(16), 2524–2544 (2022).

Biographies of the authors are not available.